Sliding planar anchoring and viscous surface torque in a cholesteric liquid crystal

Patrick Oswald,* Alain Dequidt, and Andrzej Żywociński†
Université de Lyon, Laboratoire de Physique, École Normale Supérieure de Lyon, CNRS, 46 Allée d'Italie, 69364 Lyon, France
(Received 11 January 2008; revised manuscript received 4 March 2008; published 6 June 2008)

We propose a surface treatment allowing one to obtain a sliding planar anchoring of nematic (or cholesteric) liquid crystals. It consists of depositing a thin layer of the polymercaptan hardener of an epoxy resin on an isotropic substrate (bare or ITO-coated glass plates). Microscopic observations of defect annihilations and capacitance measurements show that the molecules align parallel to the surface and slide viscously on it when they change orientation, which implies a zero (or extremely small) azimuthal anchoring energy. In contrast, the zenithal anchoring energy W_θ is found to be larger than 3×10^{-5} J/m^2. We also measured the liquid crystal rotational surface viscosity γ_S by a thermo-optical method using the large temperature variation of the pitch of a compensated cholesteric mixture. We found that the sliding length γ_S/γ_1 (where γ_1 is the bulk rotational viscosity) is very large in comparison with the length of a liquid crystal molecule. This result is explained by a simple model which takes into account the diffusion of the liquid crystal within the polymer layer.

DOI: 10.1103/PhysRevE.77.061703 PACS number(s): 61.30.Hn, 42.70.Df

I. INTRODUCTION

In a nematic liquid crystal, the rodlike molecules tend to have the same direction, their centers of mass being distributed randomly. Order is purely orientational and characterized by a unit vector $\vec{n}$ parallel to the average orientation of the molecules (with $\vec{n}\Leftrightarrow-\vec{n}$). If one adds a chiral impurity to a nematic phase, one usually obtains a cholesteric phase in which the director turns around a space direction called the helical axis [1]. The distance over which the director rotates by 2π is called the cholesteric pitch. As we shall see later, the pitch can sometimes strongly depend on temperature. One important property of these materials is their ability to be oriented by the surfaces in contact with them. In particular, considerable effort has been expended in the past to find surface treatments allowing for strong planar or homeotropic anchoring of the molecules. In the first case, the molecules orient parallel to the surface, whereas in the second case, the molecules are perpendicular to it. These two anchorings are characterized by a single direction named "surface easy axis" $\vec{n}_s$."Strong" means that the molecules shift very little from $\vec{n}_s$ when the director field is deformed in the bulk under the action of an external mechanical, electric, or magnetic torque. In this "geometric" limit, the surfaces play a passive role as they only fix the orientation of the molecules in contact with them. These boundary conditions were used in most experiments until recently and continue to play a major role in display applications. In particular, the strong planar anchoring is widely used in making the twisted or supertwisted nematic display.

Other types of anchoring exist [2]. For instance, oblique monostable or bistable anchorings have been observed on evaporated SiO layers [3] or on cleaved surfaces of crystals such as mica [4] with the possibility of passing from one to another by changing a physical parameter such as the temperature or the humidity (for a review about anchoring transitions, see chap. V of Ref. [1]). More recently, planar and oblique azimuthally degenerate anchorings have also been reported in the literature. Different techniques have been proposed to reach such boundary conditions. One of them has consisted of adding to the liquid crystal a small amount of oligomeric molecules [5]. This method was shown to lead to very small zenithal (out of substrate plane) and azimuthal (in plane) anchoring energies with the liquid crystal 4-pentyl-4′-cyanobiphenyl (5CB). Another technique consists of depositing a "thick" layer (more than 100 Å, typically) of a surfactant belonging to the family of the organofunctional silanes. One of them, the (3-glycidoxypropyl) trimethoxysilane (also called 3-GPS or GLYMO) gives a planar degenerated anchoring with the liquid crystal 5CB [6]. One can also graft on the surface highly mobile polymer chains. For instance, grafted polystyrene was shown to lead to a conically degenerated anchoring of the nematic 5CB with a pretty small zenithal anchoring energy [7]. Thin layers of the photopolymer NOA60 (Norland Optical Adhesive 60 from Epotecny) was also used recently to produce a planar anchoring with an ultraweak azimuthal anchoring [8]. These anchorings are interesting for the following two reasons:

(1) First, they open the possibility of making new and more performing displays in which the surface now plays an active role, the anchoring conditions changing when switching between two states of the display [9–11].

(2) Second, they allow one to perform experiments in the field of fundamental physics.

A good example was the first direct observation of the smectic blocks in a twist-grain boundary smectic A phase (TGB_A). In this experiment, the GLYMO surface treatment was used [12]. Another example was the experimental evidence of backflow effects during the collapse of two disclination lines [13]. In this case, the surfaces were treated with the UV glue NOA60. It must be noted that in this experiment, an electric field was used to move the lines, which shows that the anchoring was not completely sliding.

In the present paper, we describe a surface treatment we recently used to evidence the thermomechanical Lehmann

*patrick.oswald@ens-lyon.fr
†Permanent address: Department III, Institute of Physical Chemistry, Polish Academy of Sciences, Kasprzaka 44/52, 01-224 Warsaw, Poland.

effect in cholesteric liquid crystal [14,15]. This surface treatment turned out to give planar and sliding anchoring, which was essential for observing the Lehmann effect. In our case, it consisted of spin coating a thin layer of the polymercaptan hardener of an epoxy resin (Structuralit 7).

The goal of the paper is to establish the unique properties of this surface treatment as it gives a planar alignment of the molecules on the surface with a strong zenithal anchoring energy, while allowing the molecules to rotate viscously on the surface (which implies a zero or extremely small azimuthal anchoring energy). To show these results we conducted microscopic observations of defect annihilations and capacitance measurements. We also developed a thermo-optical method to determine the liquid crystal surface viscosity γ_S, a quantity difficult to measure and very little documented in the literature in comparison with the anchoring energy.

The plan of the article is the following. In Sec. II, we describe the sample preparation and we show from microscopic observation of the optical texture and from capacitance measurements that the anchoring of the molecules on the polymercaptan is planar and sliding. In Sec. III, we measure the bulk rotational viscosity γ_1 and show that the presence of the polymeric layer does not change its value. In Sec. IV, we show how to measure the surface viscosity γ_S of the liquid crystal by measuring the variations of the optical transmittance of samples of different thicknesses during temperature ramps. The measured value of γ_S is discussed within a simple model in Sec. V, while in Sec. VI, we discuss the problem of the annihilation of two $\pm 1/2$ disclination lines. Finally, conclusions are drawn in Sec. VII.

II. SAMPLE PREPARATION AND CAPACITANCE MEASUREMENTS

The liquid crystal chosen was a mixture of 4-n-octyloxy-4′-cyanobiphenyl (8OCB from Synthon Chemicals GmbH & Co.) and of cholesteryl chloride (CC from Aldrich) in proportion 1:1 in weight with a compensation point at $T_c = 59$ °C and a clearing point at 66.5 °C. We recall that at T_c, the equilibrium twist vanishes and changes sign. The phase has thus a nematiclike structure at this particular temperature. The 8OCB was purified by one of us (A.Z.) and the CC was used without further purification. The mixture was filtered in the cholesteric phase through 0.2 μm nylon filter to remove dust particles.

The samples were prepared between two glass plates treated either for strong planar unidirectional anchoring or for planar sliding anchoring.

The first anchoring is classical and was obtained by covering the surface with a rubbed polyimide layer baked at 300 °C during 2 hours (ZLI 2650 from Merck). To realize the second anchoring, we treated the surface with the polymercaptan hardener of an epoxy glue (Structalit 7 from Eleco). This polymer was first dissolved in a ketone, the 2-butanone (5% in mass of hardener). The obtained solution was then filtered through 0.2 μm teflon membrane to eliminate dust particles and spread by spin coating on the plate at 500 rpm for 1 mn. In this way, the polymercaptan hardener formed a homogeneous thin layer wetting perfectly the surface (up to 100 °C, at least). Its thickness was measured by Michelson interferometry and was found to be of the order of 0.2 μm. In addition, the layer was held at 60 °C for one hour under vacuum in order to completely evaporate the ketone. This precaution is important to not pollute the liquid crystal [16]. Finally, nickel and tungsten wires of calibrated diameters were used as spacers to fix the sample thickness.

In order to prove that this surface treatment gives a sliding planar anchoring, we performed the two following experiments. In the first one, we made a 10 μm-thick sample with the two glass plates treated with the polymercaptan hardener. The liquid crystal was first introduced by capillarity in the isotropic phase and then cooled down into the cholesteric phase. As a result we observed the formation of a "*Schlieren*" texture containing a large quantity of $\pm 1/2$ disclination lines perpendicular to the surfaces [Fig. 1(a)]. This observation clearly shows that the anchoring is planar (and not oblique) and azimuthally degenerate since it is the only orientation allowing such defects. Note that ± 1 defects are also present, but they are much less numerous than the previous ones because they cost more elastic energy [1]. In addition, we observed that isolated pairs of opposite defects were able to spontaneously annihilate [Fig. 1(b)]. This is a clear indication that the anchoring is sliding, as otherwise the defects could not move. This is compatible with a zero (or extremely small) azimuthal anchoring energy and the absence of memory effects, at least over the time scale of our experiments, i.e., 2–3 days. In this respect, our anchoring seems to be more sliding than that reported in Ref. [5] or in Ref. [13] (in this work, in particular, where the UV glue NOA60 was used, it was necessary to apply a small horizontal electric field to observe the annihilation of the defects). We also observed that defects of positive strength moved faster than defects of negative strength, in agreement with previous experiments [13,17] and theoretical works [18–20]. Finally, we emphasize that the annihilation is a slow process in spite of the sliding anchoring as long as the distance between the two defects is larger than a few tens of a micrometer. This point will be discussed in detail in Sec. VI.

To confirm that the anchoring was planar, we performed capacitance measurements. More precisely, we made two 10 μm-thick samples, the first one treated for strong planar anchoring on one plate and for sliding anchoring on the opposite one (called sample of type I in the following), whereas the second sample was treated for strong planar (and parallel) anchoring on both sides (called sample of type II in the following). In both cases, the glass plates were coated with indium-tin oxide (ITO) layers to impose the electric field. In Fig. 2, we show the capacitances of the two cells measured at the compensation temperature as a function of the applied voltage at frequency $f = 10$ kHz. In the figure, the capacitances C are normalized to their values $C_\perp$ measured below the threshold of Fredericksz instability V_c (of the order of $0.92 V_{\mathrm{rms}}$ in both samples, which proves, by the way, that the presence of polymercaptan hardener does not change the value of the splay constant K_1 as well). Within experimental errors, the two curves superimpose. In addition, measurements of the capacitances of the cells before and after filling with the liquid crystal led to similar values (within 1%) of $\varepsilon_\perp$

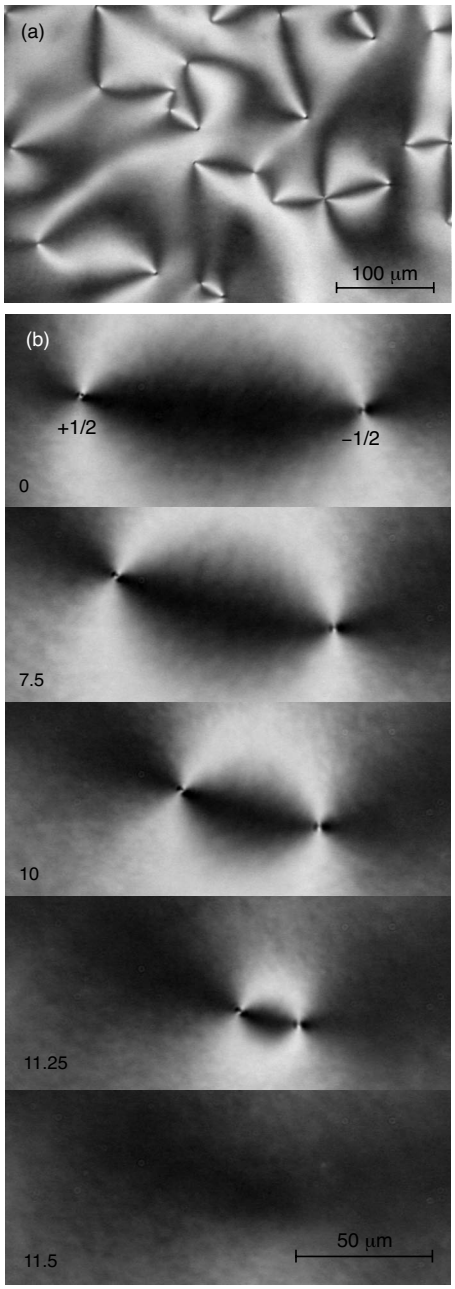

FIG. 1. (a) Texture observed at the compensation temperature after a quench from the isotropic liquid. (b) Sequence of photographs showing the spontaneous collapse at of two $\pm 1/2$ disclination lines. Note the $+1/2$ defect moves faster than the $-1/2$ defect. Time is given in min at the bottom left-hand side of the photographs. $d=10$ μm. Crossed polarizers.

(4.52 and 4.50, respectively), in very good agreement with the value given previously (4.5 ± 0.2 [14,15]).

From this experiment, we concluded that the anchoring of the liquid crystal on the polymercaptan hardener is planar and rather strong zenithally since it behaves similar to the polyimide layer up to an electric field of 2 V/μm. More precisely, we estimated a lower bound for the zenithal anchoring energy W_θ by noting that at electric field E_{max} $=2$ V/μm, the liquid crystal was not fully realigned by the field close to plate treated with the polymercaptan hardener.

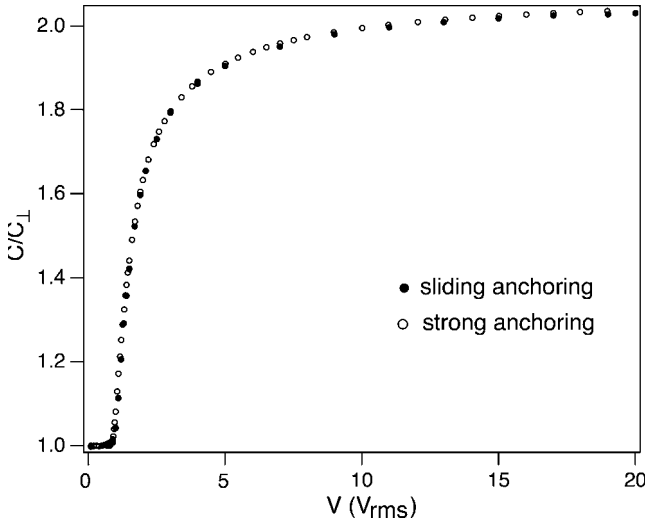

FIG. 2. Capacitance as a function of the applied voltage (f $=10$ kHz) measured at the compensation temperature T_c in a standard planar sample and in a sample treated on one plate for sliding anchoring. The curves superpose within experimental errors.

As this phenomenon occurs for electric fields larger than the saturation field $E_s=W_\theta/\sqrt{\varepsilon_0\varepsilon_a K}$ [21] (with ε_a the dielectric anisotropy and K the average of the splay and bend elastic constants), we deduced that $W_\theta > E_{max}\sqrt{\varepsilon_0\varepsilon_a K}$ since E_{max} was less than E_s experimentally. That gives $W_\theta > 3\times 10^{-5}$ J/m^2 knowing that $\varepsilon_a=5$ and $K=4.6\times 10^{-12}$ N [14,15].

III. ROTATIONAL VISCOSITY γ_1

In practice, the melting temperature of the cholesteric phase is lower by typically 1 °C in samples treated for sliding anchoring. In contrast, the compensation temperature does not change within ± 0.2 °C. This suggests that a small amount of the polymercaptan hardener dissolves in the liquid crystal. In the following section, we shall need the value of the bulk rotational viscosity γ_1. For this reason and to investigate the influence of the dissolved polymer, we measured γ_1 in planar samples of the two types (as defined in the previous section) at the compensation temperature. The method used was classical and consisted of first destabilizing the sample with a large electric field ($20V_{\rm rms}$, $f=10$ kHz) and then, of observing the relaxation of the distorted director field after the electric field was removed. In practice, the sample is placed between crossed polarizers at 45° of the anchoring direction and its optical transmittance is measured by a photodiode connected to a memory oscilloscope. Curves obtained with samples of types I and II are shown in Fig. 3. To fit these curves, we took advantage that we previously measured the elastic constants, the dielectric constants, and the optical indices of the liquid crystal at the compensation point: $K_1=3.4\times 10^{-12}$ N, $K_3=5.9\times 10^{-12}$ N, $\varepsilon_\parallel=9.4$, $\varepsilon_\perp$ $=4.5$, $n_o=1.55$, and $n_e=1.64$ [14,15]. Using these data, it was possible to solve numerically the governing equations for the director field (in anisotropic elasticity) and to then calculate the optical transmittance. We took as fit parameters the sample thickness d and the classical relaxation time $\tau=\frac{\gamma_1 d^2}{\pi^2 K_1}$.

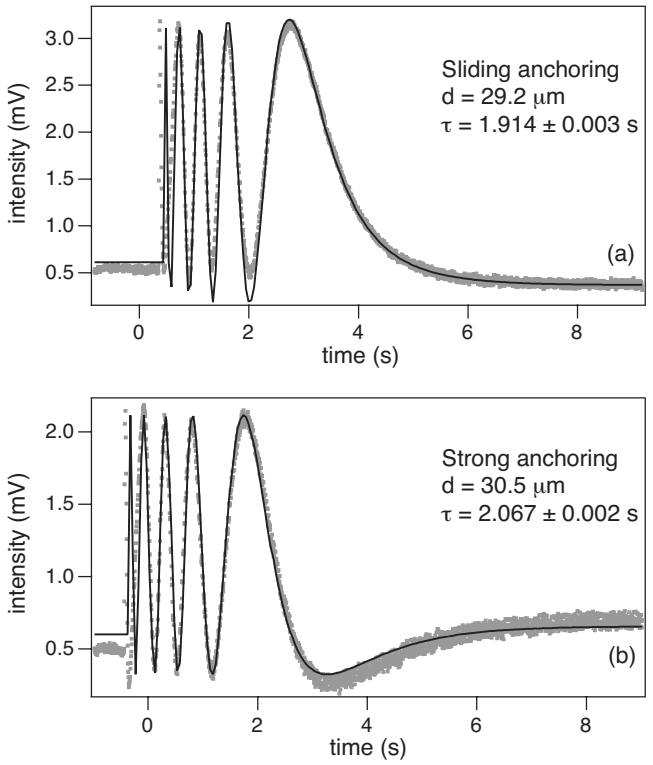

FIG. 3. Optical transmittance measured at $T=T_c$ between crossed polarizers at 45° of the anchoring direction as a function of time after switching off the voltage. Points are experimental and correspond to several curves measured at different places in the sample. The solid line is the best fit to the numerical model. (a) Type I sample; (b) type II sample.

Two fits are shown, respectively, in Fig. 3(a) for a type I sample and in Fig. 3(b) for a type II sample. In the first case, we found $d=29.2$ μm and $\tau=1.91$ s, while $d=30.5$ μm and $\tau=2.07$ s in the second sample. In these two examples, the fitted thickness was very close to the nominal one (30 μm). We thus calculated γ_1 by taking the value of the thickness given by the fit and $K_1=3.4\times10^{-12}$ N [14,15]. This procedure gave the same value in type I and type II samples: $\gamma_1=0.075\pm0.009$ Pa s. We performed similar measurements in 20 μm-thick commercial type II cells (from Instec, Inc.) and found again a similar value within experimental errors.

In conclusion, the rotational viscosity γ_1 does not change in a measurable way in the presence of the polymercaptan hardener. This result agrees with previous conclusions of Jǎkli *et al.* [22] about the role in the value of γ_1 of a polymer dissolved in the liquid crystal. In the following, we shall take $\gamma_1=0.075\pm0.009$ Pa s.

IV. SURFACE VISCOSITY γ_S

In practice, the director does not rotate freely at the surface of the liquid polymercaptan layer, but experiences a viscous surface torque which can be written in the usual form [23]

$$\vec{\Gamma}_S=-\gamma_S\vec{n}\times\frac{\partial\vec{n}}{\partial t}. \tag{1}$$

The surface viscosity γ_S has the dimension of a bulk viscosity times a length. This length l_S characterizes the distance over which the liquid crystal interacts with the polymer layer. It will be discussed in Sec. V. In the next three sections, we successively describe the principle of the experiment, the technique of measurements, and the experimental results.

A. Principle of the experiment

The experiment consisted of measuring the optical transmittance in monochromatic light ($\lambda=546$ nm) of a type I sample as a function of the temperature when it was changed at a constant rate. The sample was placed between crossed polarizer and analyzer with the polarizer parallel to the anchoring direction imposed on the lower glass plate. Due to the sliding anchoring on the upper plate, the transmittance changed with the temperature and vanished (by assuming an adiabatic rotation of the plane of polarization of the light) when the director on this surface was perpendicular to the analyzer. We checked numerically that this optical condition was fulfilled at a temperature T_0 (close to T_c) being a function of the imposed temperature ramp $r=dT/dt$ (with $T_0\rightarrow T_c$ when $r\rightarrow0$). The experiment thus consisted of measuring $T_0(r)$ in samples of different thicknesses d. In the following, we show that the derivative dT_0/dr is a well-defined function of d, γ_1, and γ_S.

In order to calculate this quantity, we first recall the governing equations of the problem. Let φ be the angle between the director and the anchoring direction on the bottom plate. Because the director remains parallel to the glass plates, it is only function of z and t (with the z axis perpendicular to the plates). If, in addition, the temperature and thus, the equilibrium twist q, can be supposed independent of z, an assumption we shall justify in the Appendix, then the bulk torque equation simply reads

$$\gamma_1\frac{\partial\varphi}{\partial t}=K_2\frac{\partial^2\varphi}{\partial z^2}. \tag{2}$$

At the bottom plate, the director orientation is fixed, so that

$$\varphi=0 \quad \text{at } z=0 \tag{3}$$

while at the top plate, the anchoring is sliding, imposing

$$\gamma_S\frac{\partial\varphi}{\partial t}=-K_2\left(\frac{\partial\varphi}{\partial z}-q[T(t)]\right) \quad \text{at } z=d, \tag{4}$$

where $q[T(t)]$ is the equilibrium twist of the cholesteric.

Experimentally, we impose a constant temperature ramp $r=dT/dt$, so that

$$T(t)=T_c+rt. \tag{5}$$

In addition, we know from previous measurements that q is, to a very good approximation, proportional to $T-T_c$ in the vicinity of the compensation point [14,15]. This allows us to write that

$$qd = \omega t \quad \text{with } \omega = rd\frac{dq}{dT}. \tag{6}$$

Let us now define the angle $\delta(z,t)=\varphi(z,t)-qz$ characterizing the shift to the perfect helix. According to Eqs. (1) and (6), this angle must satisfy the following equation:

$$\gamma_1 \frac{\partial \delta}{\partial t} = K_2 \frac{\partial^2 \delta}{\partial z^2} - \gamma_1 \omega \frac{z}{d}. \tag{7}$$

In the stationary regime (δ independent of t), this equation has the general solution

$$\delta = \frac{\omega}{3\omega_b}\left(\frac{z}{d}\right)^3 + az + b, \tag{8}$$

where $\omega_b = \frac{2K_2}{\gamma_1 d^2}$ is a bulk relaxation rate.

Constants b and a are, respectively, given by the boundary conditions (3) and (4),

$$b = 0 \quad \text{and} \quad a = -\frac{\omega}{d}\left(\frac{1}{\omega_b} + \frac{1}{\omega_S}\right), \tag{9}$$

where $\omega_S = \frac{K_2}{\gamma_S d}$ is a surface relaxation rate. Coming back to angle φ, the general solution reads in the stationary regime

$$\varphi = \frac{\omega}{3\omega_b}\left(\frac{z}{d}\right)^3 + \omega\left[t - \left(\frac{1}{\omega_b} + \frac{1}{\omega_S}\right)\right]. \tag{10}$$

Close to T_c, the optical transmittance vanishes when $\varphi(d,t)=0$. This condition is fulfilled at time $t_0 = \frac{1}{\omega_S} + \frac{2}{3\omega_b}$ corresponding to temperature $T_0 = T_c + r(\frac{1}{\omega_S} + \frac{2}{3\omega_b})$ according to Eq. (6).

Finally we obtain the researched quantity

$$\frac{dT_0}{dr} = \frac{1}{\omega_S} + \frac{2}{3\omega_b} = \frac{\gamma_S}{K_2} d + \frac{\gamma_1}{3K_2} d^2. \tag{11}$$

In the following section, we show how to measure this quantity.

B. Experiment

We used a Mettler oven to impose temperature ramps to the samples. The oven was placed on the stage of a polarizing Leica microscope and the optical transmittance was measured with a photodiode. To measure the temperature of the sample we used a local sensor consisting of a 10 μm in diameter tungsten wire placed between the two glass plates a few mm apart from the zone of interest. Its resistance was measured via a four-wire method with a Keihtley 2001 multimeter interfaced with a personal computer (PC) and was found to linearly depend on the temperature. The temperature stability of this home-made sensor was excellent as no visible drift was observed over many days. An example of a measured temperature profile is shown in Fig. 4. For slow ramps (inferior to 3 °C/min in absolute value), we found very good agreement between nominal and measured values. For faster ramps, small differences were observed. For this reason, we measured systematically the temperature ramp to minimize errors.

An attentive reader could object that the temperature measured in this way could be different from the temperature in the middle of the sample where optical measurements were performed. For this reason, we realized a dummy sample with one wire on the side (as in usual samples) and another in the middle. We then recorded as a function of time the temperatures given by the two wires with a Keihtley 2001 multimeter equipped with a scanner card. In Fig. 5 we plotted the temperature of the side sensor as a function of the temperature of the middle sensor. Four curves are shown corresponding to two pairs of ramps of opposite signs. The two curves corresponding to the ±2 °C/min ramps superimpose perfectly (within the experimental noise); by contrast, a systematic small shift (certainly depending on the thermal contact between the sample and the oven, but always within ±0.1°) was often detected for the fastest ramps (±7 °C/min). This test proved that our sensor did give the temperature of the sample at the place where measurements were performed with a negligible error for slow ramps and

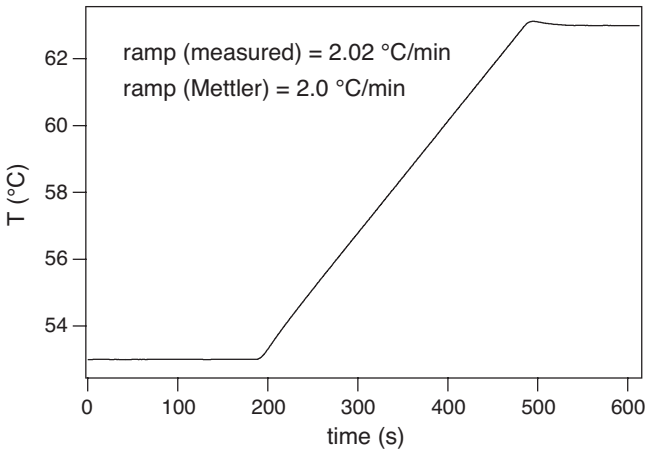

FIG. 4. Temperature profile measured *in situ* with the tungsten wire. The measured value of the temperature ramp is here slightly larger than its nominal value given by the Mettler oven. This difference increases when the ramp is faster, but never exceeds 5%.

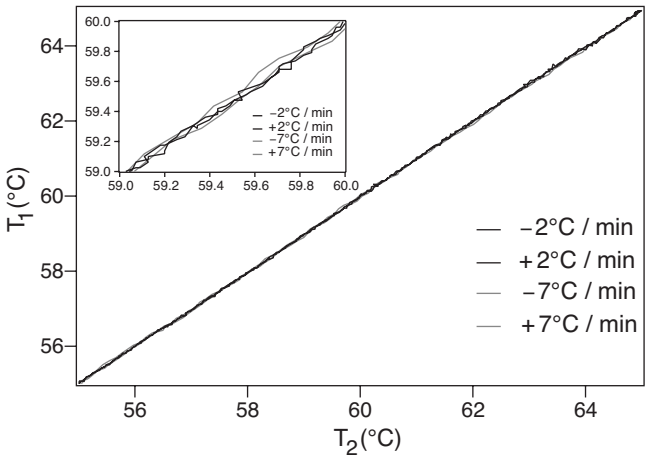

FIG. 5. Temperature of the side wire as a function of the temperature of the middle wire. The curves measured at ±2 °C/min are superimposed (within the experimental noise) whereas those measured at ±7 °C/min are systematically shifted by about 0.1 °C. Note that these curves are noisier than in Fig. 4 because of the use of the scanner card.

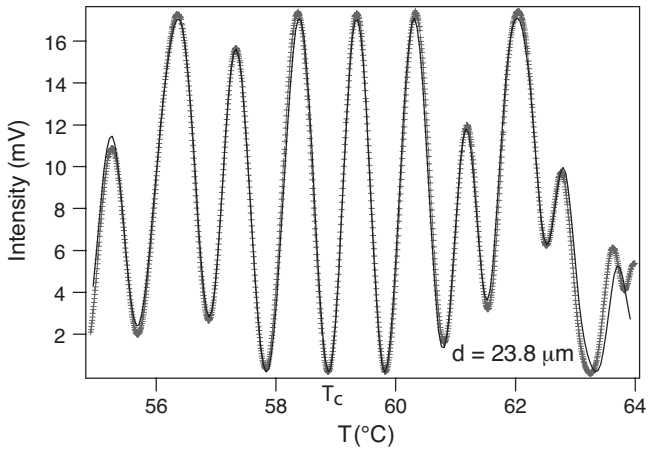

FIG. 6. Optical transmittance between crossed polarizers as a function of temperature. The temperature ramp was 0.2 °C/min. Points are experimental and the solid line is the best fit to Eq. (12).

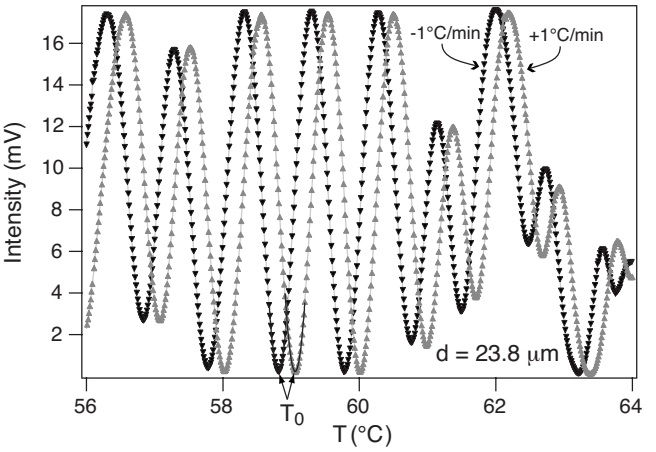

FIG. 7. Curves of optical transmittance measured between crossed polarizers as a function of temperature for two ramps of equal amplitude, but opposite signs. Temperatures T_0 are obtained by fitting with parabolas (solid lines) the local minima.

an error that does not exceed ±0.1 °C for the fastest ramps.

The next step was to determine for each sample its compensation temperature. The used method consisted of recording its optical transmittance as a function of temperature under a very slow temperature ramp (typically 0.2 °C/min). Note we used two Keihtley multimeters interfaced with a PC to record the photodiode voltage (proportional to the optical transmittance) and the temperature given by the tungsten wire. At this speed, the cholesteric phase may be considered at equilibrium during the ramp and its optical transmittance is given by the following formula:

$$\frac{I}{I_0} = \frac{1}{2} - \cos(2qd)\frac{\kappa^2 + \cos(2qd\sqrt{1+\kappa^2})}{2(1+\kappa^2)} - \sin(2qd)\frac{\sin(2qd\sqrt{1+\kappa^2})}{2\sqrt{1+\kappa^2}}, \quad (12)$$

with $\kappa = \frac{\pi\Delta n}{q\lambda}$ ($\lambda = 546$ nm).

A typical experimental curve is shown in Fig. 6. To fit it to the previous law, we chose as free parameters the compensation temperature T_c (knowing that the equilibrium twist is given by $q(\mu m^{-1}) = 0.1365(T - T_c) + 0.00284(T - T_c)^2$, with the temperatures in °C [14,15]), the sample thickness d, the intensity I_0, and the birefringence [which we took in the form $\Delta n = a - b(T - T_c)$]. This led to $T_c = 58.9$ °C, $I_0 = 16.9$ mV, $d = 23.8$ μm, and $\Delta n = 0.090 - 0.0029(T - T_c)$. Note that these values of the thickness and of the birefringence at the compensation point are very close to the expected ones: 25 μm for the thickness and 0.09 for the birefringence [14,15]. In the following, we took for the thickness the value given by the fit.

Once the compensation temperature and the thickness of a sample were measured, we systematically recorded its transmittance curves for different temperature ramps. Two curves measured for two successive ramps of opposite signs are shown in Fig. 7. As expected the curve obtained by cooling is shifted to the left (towards lower temperatures), while the other obtained by heating is shifted to the right (towards higher temperatures). From these curves, we measured temperatures $T_0(r)$ by fitting the corresponding minima of the transmittance curve with parabolas (see in Fig. 7). Curve $T_0(r)$ is shown in Fig. 8. It is well fitted by a linear law the slope of which gives the researched quantity dT_0/dr defined in Eq. (11). The experiment was then repeated for samples of different thicknesses. Our results are given in the next section.

C. Results

Figure 9 collects all our experimental results obtained with samples of thicknesses ranging between 7 and 33 μm. In practice, it was not really possible to perform the experiment with thicker samples because of a spontaneous destabilization of the helical structure into cholesteric fingers when the temperature was changed (even as slowly as ±1 °C/min).

In order to find the value of the surface viscosity, we fitted this experimental curve to the theoretical law, Eq. (11), by taking for the value of the bulk rotational viscosity γ_1 that

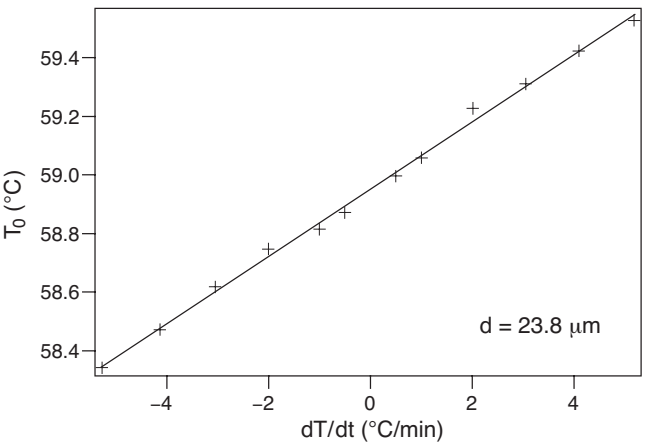

FIG. 8. Temperature T_0 as a function of the temperature ramp r for a sample of a given thickness and its fit to a linear law.

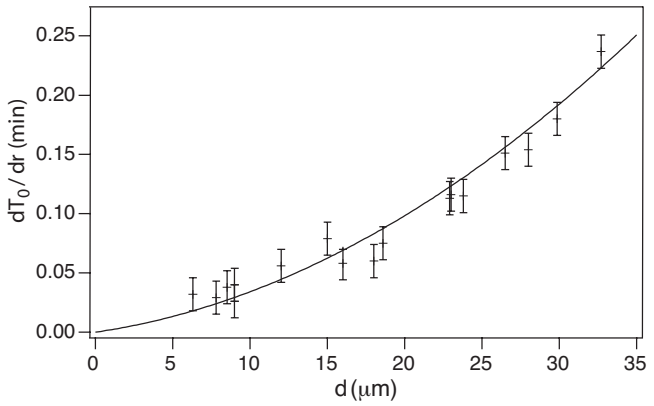

FIG. 9. Derivative dT_0/dr as a function of the sample thickness d. The solid line is the best fit to Eq. (11) by taking $\gamma_1 = 0.075$ Pa s.

measured previously, 0.075 ± 0.009 Pa s and for the twist constant $K_2 = 2.8 \pm 0.2 \times 10^{-12}$ N [14,15]. In this way, we found from the fit of the experimental data and by taking into account the uncertainties in the values of γ_1 and K_2,

$$\gamma_S = 3.2 \pm 0.8 \times 10^{-7} \text{ Pa s m}.$$

This value is discussed in the next section.

V. SIMPLE MODEL FOR THE SURFACE VISCOSITY

This value of the surface viscosity is very large. Indeed, let us consider the viscosity η of the polymercaptan hardener. Measurements in a rotating rheometer gave $\eta \sim 1$ Pa s at the compensation temperature (59 °C) for shear rates ranging between 0.1 and 10 s^{-1}. From these two quantities, we can form a length

$$l_S = \frac{\gamma_S}{\eta}, \tag{13}$$

which turns out to be very large, of the order of 0.3 μm. This value is of the same order of magnitude as the thickness l_P of the polymer layer we measured by Michelson interferometry.

This result thus suggests that the liquid crystal diffuses into the polymer layer over a typical distance l_D. This distance must be smaller than l_P in order that the liquid crystal molecules do not adsorb on the glass (no memory effects were observed over many days on condition that the polymercaptan layer be thick enough [24]).

To estimate l_D, let us assume that each molecule dissolved in the polymer layer experiences a viscous torque Γ_{mol} proportional to its rotational velocity $\dot{\varphi}$. For a rodlike molecule of length L and diameter Φ, the viscous torque reads [25]

$$\Gamma_{mol} = \frac{\pi \eta L^3 \dot{\varphi}}{3[\ln(L/\Phi) - 0.8]}. \tag{14}$$

Let n_S be the number of molecules dissolved in the polymer layer per unit surface area. In a crude model, the surface torque Γ_S introduced phenomenologically in Eq. (1) reads

$$\Gamma_S \sim n_S \Gamma_{mol}, \tag{15}$$

which gives the surface viscosity

$$\gamma_S \sim n_S \frac{\pi \eta L^3}{3[\ln(L/\Phi) - 0.8]}. \tag{16}$$

Finally, writing that $l_D \sim n_S L \Phi^2$, we obtain from the preceding equation

$$l_D \sim \frac{\gamma_S}{\eta} \left(\frac{\Phi}{L}\right)^2 \left[\ln\left(\frac{L}{\Phi}\right) - 0.8\right]. \tag{17}$$

In practice $L \sim 30$ Å, $\Phi \sim 5$ Å, which gives from the measured value of γ_S and η given before, $l_D \sim 0.01$ μm $= 100$ Å. As expected, we find that l_D is smaller than the thickness of the polymer layer, although this calculation obviously underestimates its value.

To summarize, the large value of l_S defined in Eq. (13) is certainly a clear indication that the nematic liquid crystal dissolves partially in the polymer surface layer. On the other hand, l_D must be smaller than the thickness of the polymer layer in order to prevent that the liquid crystal molecules adsorb on the glass. These conclusions are very similar to those drawn before by Vilfan *et al.* [26], who also measured by dynamic light scattering very large values of l_S for the liquid crystal 5CB in contact with a photoaligning poly-(vinyl-cinnamate) layer.

VI. ANNIHILATION TIME OF TWO DISCLINATION LINES OF OPPOSITE SIGNS

Before concluding the article, let us return to the problem of the annihilation of the two $\pm 1/2$ disclination lines shown in Fig. 1(b). Indeed, their annihilation may seem too long as it takes about 11.5 min while the initial distance between the two defects is of "only" 110 μm. Thus, one may wonder whether this observation is compatible with a fully sliding anchoring.

To show it is indeed the case, let us estimate this time. A straightforward calculation neglecting the backflow effects and the material elastic anisotropy gives

$$t_{annihil} = \frac{\gamma_1^\star}{4K} r_0^2 \ln \frac{r_0}{r_c}, \tag{18}$$

where r_0 is the initial distance between the two defects, r_c a core radius of molecular size, $K = \frac{K_1 + K_3}{2}$ the average of the splay and bend constants, and $\gamma_1^\star$ an effective viscosity taking into account the surface viscosity $\gamma_1^\star = \gamma_1 + 2\gamma_S/d$. With the experimental values $d = 10$ μm, $r_0 = 110$ μm, $K = 4.6 \times 10^{-12}$ N [14,15], $\gamma_1 = 0.075$ Pa s, and $\gamma_S = 3.2 \times 10^{-7}$ Pa s m, we calculate $t_{annihil} \approx 16$ min by taking $r_c \approx 50$ Å.This time is longer than that observed experimentally (11.5 min). This difference is nevertheless not surprising as we know from numerical simulations that backflow effects tend to reduce by a typical factor of 1.5 the annihilation time between the two defects [18,20]. This interpretation is reinforced by the important experimental fact that the $+1/2$ defect moves faster than the $-1/2$ defect, another phenomenon predicted by the theory [18–20]. We thus conclude that our observations on defect annihilation are compatible with a sliding anchoring of the molecules on the polymer layer.

VII. CONCLUSION

We have described a surface treatment which allows us to obtain a sliding anchoring of the molecules of a compensated cholesteric mixture. We checked experimentally that this anchoring was efficient for other liquid crystals such as 5CB and 8CB, but we did not performed systematic measurements with these materials. By using the large variation of the cholesteric pitch around the compensation point, we were able to measure the surface viscosity of the liquid crystal. We emphasize that this experiment was made possible owing to the development of temperature sensors able to measure *in situ* the sample temperature. We have found that the surface viscosity γ_S was large, which we interpreted by assuming that the liquid crystal diffuses within the polymer layer over a characteristic length l_D much larger than a molecular length. This contrasts with usual surface treatments (as, for instance, bare glass or covered with a SiO or a polymerized polyvinyl alcohol or polyimide layer) where l_D, or more precisely l_S (defined in this case as the ratio γ_S/γ_1), is of the order of a molecular length [27]. In the latter case, the origin of the surface viscosity is certainly very different and was explained as due to a backflow effect close to the surface [28]. Nevertheless this explanation cannot apply here as we are dealing with azimuthal (and not zenithal) molecular rotations. As a consequence, we only have twist deformations which do not generate any backflow. Finally, note that all our experiments were performed in the stationary regime (i.e., at times $t \gg 1/\omega_b$ and $1/\omega_S$), which allowed us to escape the complications caused by the incompatibility (at the initial time, when the ramp is started) between the bulk equation (2) and the surface equation (4) [29].

One of our objective in the future will be to improve the model of the surface viscosity. This could be done by using a tensorial description [30] of the Ericksen-Leslie theory of the nematohydrodynamics coupled with a Cahn-Hilliard description [31] of the nematic-polymer interface [32]. It would also be interesting for applications to better determine the zenithal anchoring energy, for instance, by measuring the saturation voltage above which the director is fully realigned by the field. Another crucial point for applications would be to study aging properties of this anchoring over longer period of time than two or three days in order to check whether memory effects develop at long time. Such studies are planned in the future, in particular as a function of the thickness of the polymercaptan layer.

ACKNOWLEDGMENT

This work has been supported by the Polonium Program No. 11622QC.

APPENDIX

In our experiments, the average sample temperature changes quickly during the steepest ramps. As a consequence the temperature can no longer be considered as constant along the z axis. In these conditions Eq. (2) is only approximate because it neglects the spatial variations of K_2 and q. As in practice K_2 changes much less rapidly than q, we shall only consider the q variation assuming K_2=constant. In these conditions, a term proportional to $\partial q/\partial z$ occurs in the bulk torque equation (2) which becomes

$$\gamma_1 \frac{\partial \varphi}{\partial t} = K_2 \frac{\partial^2 \varphi}{\partial z^2} - K_2 \frac{\partial q}{\partial z}. \tag{A1}$$

In order to determine whether the term $-K_2 \frac{dq}{dz}$ is pertinent, let us calculate its order of magnitude with respect to the two others by using the simplified solution given by Eq. (10). By denoting by ΔT the typical temperature variation across the sample thickness d, we find

$$\gamma_1 \frac{\partial \varphi}{\partial t} = \gamma_1 \omega = \gamma_1 d \frac{dq}{dT} \frac{\partial T}{\partial t}, \tag{A2}$$

while

$$K_2 \frac{\partial q}{\partial z} = K_2 \frac{dq}{dT} \frac{\partial T}{\partial z} \approx K_2 \frac{dq}{dT} \frac{\Delta T}{d}. \tag{A3}$$

Inside the sample, the temperature satisfies the heat equation

$$\frac{\partial T}{\partial t} = D_T \frac{\partial^2 T}{\partial z^2}, \tag{A4}$$

where D_T is the thermal diffusivity of the liquid crystal. From this equation, we find that in order of magnitude

$$\frac{\partial T}{\partial t} = D_T \frac{\Delta T}{d^2}. \tag{A5}$$

This allows us to calculate the ratio between the two terms,

$$\frac{\gamma_1 \frac{\partial \varphi}{\partial t}}{K_2 \frac{\partial q}{\partial z}} \approx \frac{\gamma_1 d \frac{dq}{dT} D_T \frac{\Delta T}{d^2}}{K_2 \frac{dq}{dT} \frac{\Delta T}{d}} = \frac{D_T}{D_o}, \tag{A6}$$

where $D_o = \frac{K_2}{\gamma_1}$ is the orientational diffusivity. In our sample, $D_o \approx 3.7 \times 10^{-11}$ m^2 s^{-1}. As for its thermal diffusivity, it must be of the same order of magnitude as in usual nematics, $D_T \approx 10^{-7}$ m^2 s^{-1} [33,34]. From these two values we can estimate that

$$\frac{\gamma_1 \frac{\partial \varphi}{\partial t}}{K_2 \frac{dq}{dz}} \approx 3000. \tag{A7}$$

This fully justifies neglecting the term in $\frac{dq}{dz}$ in the bulk torque equation.

[1] P. Oswald and P. Pieranski, *Nematic and Cholesteric Liquid Crystals: Concepts and Physical Properties Illustrated by Experiments* (Taylor & Francis, Boca Raton, 2005).
[2] B. Jérôme, Rep. Prog. Phys. **54**, 391 (1991).
[3] B. Jérôme, P. Pieranski, and M. Boix, Europhys. Lett. **5**, 693 (1988).
[4] J. Bechhoefer, B. Jérôme, and P. Pieranski, Phys. Rev. A **41**, 3187 (1990).
[5] G. P. Bryan-Brown, E. L. Wood, and I. C. Sage, Nature (London) **399**, 338 (1999).
[6] I. Dozov, D. N. Stoenescu, S. Lamarque-Forget, P. Martinot-Lagarde, and E. Polossat, Appl. Phys. Lett. **77**, 4124 (2000).
[7] O. O. Ramdane, P. Auroy, S. Forget, E. Raspaud, P. Martinot-Lagarde, and I. Dozov, Phys. Rev. Lett. **84**, 3871 (2000).
[8] M. Nespoulos, C. Blanc, and M. Nobili, J. Appl. Phys. **102**, 073519 (2007).
[9] I. Dozov, M. Nobili, and G. Durand, Appl. Phys. Lett. **70**, 1179 (1997).
[10] L. Komitov, J. Yamamoto, and H. Yokoyama, J. Appl. Phys. **89**, 7730 (2001).
[11] L. Komitov, B. Helgee, J. Felix, and A. Matharu, Appl. Phys. Lett. **86**, 023502 (2005).
[12] D. N. Stoenescu, H. T. Nguyen, P. Barois, L. Navailles, M. Nobili, P. Martinot-Lagarde, and I. Dozov, Mol. Cryst. Liq. Cryst. Sci. Technol., Sect. A **358**, 275 (2001).
[13] C. Blanc, D. Svenšek, S. Žumer, and M. Nobili, Phys. Rev. Lett. **95**, 097802 (2005).
[14] A. Dequidt and P. Oswald, Europhys. Lett. **80**, 26001 (2007).
[15] A. Dequidt, A. Żywociński, and P. Oswald, Eur. Phys. J. E **25**, 277 (2008).
[16] We would like to emphasize that the decrease of 3–4 °C of the melting temperature reported in Ref. [15] was mainly due to a pollution of the liquid crystal by the ketone.
[17] P. Oswald and J. Ignés-Mullol, Phys. Rev. Lett. **95**, 027801 (2005).
[18] G. Toth, C. Denniston, and J. M. Yeomans, Phys. Rev. Lett. **88**, 105504 (2002).
[19] E. I. Kats, V. Lebedev, and S. V. Malinin, J. Exp. Theor. Phys. **95**, 714 (2002).
[20] D. Svenšek and S. Žumer, Phys. Rev. Lett. **90**, 155501 (2003).
[21] J. Nehring, A. R. Kmetz, and T. J. Scheffer, J. Appl. Phys. **47**, 850 (1976).
[22] A. Jǎkli, D. R. Kim, M. R. Kuzma, and A. Saupe, Mol. Cryst. Liq. Cryst. **198**, 331 (1991).
[23] P. G. de Gennes, *The Physics of Liquid Crystals* (Clarendon Press, Oxford, 1974), p. 97.
[24] Samples prepared by using a concentration of 2% in mass of hardener in the ketone showed clear memory effects after one day at the compensation temperature. In this case, the planar anchoring was memorized on the plate treated for sliding anchoring and a weak azimuthal anchoring energy was occurring as in Ref. [8].
[25] R. G. Larson, *The Structure and Rheology of Complex Fluids* (Oxford University Press, Oxford, 1999).
[26] M. Vilfan, I. D. Olenik, A. Mertelj, and M. Čopič, Phys. Rev. E **63**, 061709 (2001).
[27] A. Mertelj and M. Čopič, Phys. Rev. E **61**, 1622 (2000).
[28] G. E. Durand and E. G. Virga, Phys. Rev. E **59**, 4137 (1999).
[29] A. M. Sonnet, E. G. Virga, and G. E. Durand, Phys. Rev. E **62**, 3694 (2000).
[30] T. Qian and P. Sheng, Phys. Rev. E **58**, 7475 (1998).
[31] J. W. Cahn, Trans. Metall. Soc. AIME **242**, 166 (1968).
[32] V. Popa-Nita and P. Oswald, J. Chem. Phys. **127**, 104702 (2007).
[33] W. Urbach, H. Hervet, and F. Rondelez, Mol. Cryst. Liq. Cryst. **46**, 209 (1978).
[34] G. Ahlers, D. S. Cannell, L. I. Berge, and S. Sakurai, Phys. Rev. E **49**, 545 (1994).